

Comparative Analysis of Optimized Signals for Satellite Navigation Systems

Fabio Dovis, Letizia Lo Presti

Politecnico di Torino, Electronic Department - Italy
 Email: fabio.dovis@polito.it
letizia.lopresti@polito.it

Maurizio Fantino, Paolo Mulassano

Istituto Superiore Mario Boella (ISMB) – Italy
 Email: maurizio.fantino@ismb.it
paolo.mulassano@ismb.it

Abstract— Recently the Multiplexed Binary Offset Carrier (MBOC) has been proposed as a possible modulation with improved performance for the future signals to be broadcast by the Global Positioning System (GPS) and Galileo. Such a proposed signal will be adopted by the GPS L1C and the Galileo E1 Open Service (OS) signals [1].

The MBOC power spectral density is a mixture of BOC(1,1) spectrum and BOC(6,1) but since different time waveforms can be combined to produce a MBOC like spectrum, this does not strictly imply that the same time signals will be adopted for Galileo and GPS. This paper presents the results of the analysis conducted by the authors related to the acquisition and tracking performance of the Composite BOC (CBOC) modulations. The CBOC(6,1,1/11) and CBOC(6,1,4/33) are considered and compared to the baseline BOC(1,1). The performance have been obtained employing a fully software receiver developed by the authors, able to process any Galileo and/or GPS signals and other possible signals modifications.

I. INTRODUCTION

With the aim of assuring the coexistence of Galileo with Global Positioning System (of present and future generation), the European Commission (EC) and Unites States of America (USA) reached an agreement on the compatibility and interoperability between the two systems in June 2004. Such an agreement clearly stated as central point that the common signal baseline structure for the open access GPS and Galileo signals at the L1 band is the BOC(1,1) modulation. The *Binary Offset Carrier* (BOC) modulation is a signal obtained by direct multiplication of a Binary Phase Shift Keying modulated signal (spreading code) and a squared subcarrier. A BOC (n,m) signal is then characterized by two parameters, the sub-carrier frequency and the rate of the spreading code. Conventionally n and m are two integer numbers representing respectively:

- the subcarrier frequency in multiples of 1.023 MHz
- the chip rate in multiples of 1.023 Mcps

In a certain sense the L1 carrier of GPS and the C/A code rate are taken as “fundamental” frequency and rate for the construction of novel navigation signals.

In this case the general BOC(n,m) signal can be written as

$$s(t) = \sqrt{P} \sum_{i=-\infty}^{+\infty} \left\{ c_i d_i r \left(t - i \frac{T_R}{m} \right) \text{sign} \left[\sin \left(2\pi \frac{n}{T_R} t \right) \right] \right\} \quad (1)$$

where $f_R = \frac{1}{T_R} = 1.023 \text{ MHz}$, c_i is the sequence of the code

chips values, d_i are the data and $r(t)$ is a rectangular pulse shape of unitary amplitude and of duration Tr/m .

The signal

$$s_{\text{sin}}(t) = \text{sign} \left[\sin \left(2\pi \frac{n}{T_R} t \right) \right] \quad (2)$$

represents the subcarrier. When not differently specified the subcarrier as to be intended as a squared sine waveform with a fundamental frequency $f_{sc} = \frac{1}{T_{sc}} = \frac{n}{T_r}$.

The agreement between EC and USA on the BOC(1,1) as the baseline for the L1 carrier frequency, also underlined that such common signal could be optimized by both parties in order to achieve better performance. Thus, EC and USA started to analyze possible innovative modulation strategies [3] in view of Galileo optimization and for the future new generation of GPS signals.

According to the recent activities carried out by the Galileo Signal Task Force (STF), it comes out that the Multiplexed Binary Offset Carrier (MBOC) could be a good candidate for both GPS and Galileo satellites for the L1 band, and a further agreement has been signed by both parties [2].

The MBOC signal is defined in the frequency domain as a mixture of the BOC(1,1) spectrum and of the BOC(6,1) spectrum and it is considered a good candidate for the Galileo E1 Open Service (OS) signal and for the GPS L1C signal. Since different time waveforms can be combined to produce a MBOC like spectrum, this does not strictly imply that the same signal format will be adopted for Galileo and GPS.

The additional contribution of the BOC(6,1) spreading signal in the spectrum aims at increasing the amount of the power at higher frequency, which leads to time signal with narrower correlation functions and then with associated better performance in terms of signal tracking and multipath rejection.

Several parameters must be considered in the optimization process of Global Navigation Satellite Systems (GNSS) Signals-In-Space (SIS); an optimized signal must allow the receiver to identify the presence or the absence of a certain satellite, its ability to maintain an unambiguous signal tracking from which the determination of the pseudo-range measurement is derived and eventually the SIS must embed the robustness against intentional and not-intentional threats like any kind of interference or signal distortions (e.g. by multipath affected environments).

Regarding the signal acquisition, the optimized signal has been designed with the aim to preserve the possibility to acquire the new modulations employing the same engine structure as in the case of the BOC(1,1). Moreover, it has to be remarked that the decision of having or not a secondary code on the new MBOC Galileo SIS (as in the case of the present BOC(1,1) baseline) is not yet frozen.

Section II will describe the implementation of a Composite-BOC (CBOC) signal, which represents a possible implementation of the MBOC signal, and its characteristics will be described in Section III.

Section IV will analyze the acquisition performance obtained using the Galileo acquisition engine presented in [4] which works on a pilot channel with a potential secondary code, that further modulates the primary pseudo-random sequences (any kind of BOC or MBOC).

The Tracking performance of the possible MBOC implementation for different possible CBOC choices will be presented in Section V assessing the impact of the new optimized modulation on systems tailored to the BOC(1,1) signal in terms of compatibility and interoperability.

In order to evaluate the tradeoff between the increased complexity and the robustness in hars environments, multipath performance results are discussed in Section VI. Finally, Section VII will draw some conclusions.

II. CBOC OPTIMIZED WAVEFORM FOR GALILEO E1 AND GPS L1C

As proposed in [2] [5] the MBOC power spectral density is a mixture of BOC(1,1) spectrum and BOC(6,1) spectrum (pilot and data channel components together). The working group proposal is to use an MBOC(6,1,1/11). The term (6,1) refers to the BOC(6,1) and the ratio 1/11 represents the power repartition of the BOC(1,1) and BOC(6,1) spectrum components as given by Equation (3)

$$G_{MBOC}(f) = \frac{10}{11}G_{BOC(1,1)}(f) + \frac{1}{11}G_{BOC(6,1)}(f) \quad (3)$$

where $G_{BOC(m,n)}(f)$ is the unit-power spectrum density of a sine-phased BOC modulation defined in [6].

Figure 1 shows the comparison among the Power Spectral Densities (PSD) of the BOC(1,1) and the possible MBOC implementation foreseen for the Galileo E1 signal: the MBOC(6,1,1/11). From the picture it is quite evident the increase in higher frequency of the MBOC(6,1,1/11) power compared to the baseline BOC(1,1) solution; this feature, as it will be highlighted in the following, will lead to sharper code correlation peaks.

MBOC modulations are defined from the power spectrum, which means that the possible time implementations which fit the definition are different.

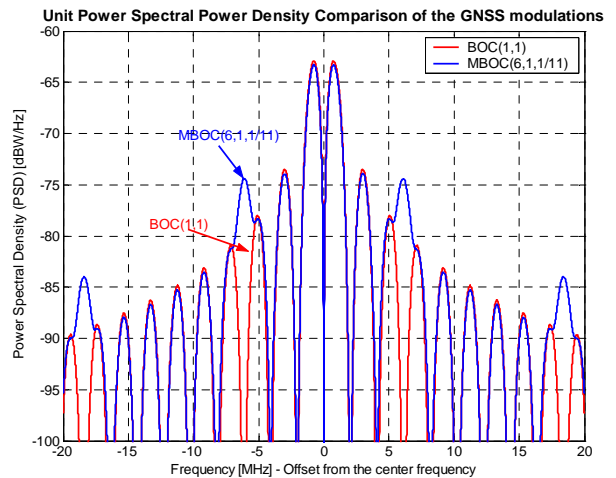


Figure 1 Unit Power Spectral Densities comparison of BOC(1,1) and MBOC(6,1,1/11)

Two different approaches to obtain a MBOC modulation have been proposed and studied [1]: the Time Multiplex BOC (TMBOC) and the CBOC.

III. CBOC FEATURES

CBOC is one of the possible strategies to obtain a power spectrum of a MBOC modulation as defined in Equation (3). The main idea is to modulate every pseudo random (PRN) code by a weighted combination of a BOC(1,1) and a BOC(6,1) spreading symbols defined as in the following:

$$s_{BOC(1,1)}(t) = \begin{cases} \text{sign}[\sin(2\pi/T_C)] & 0 \leq t \leq T_C \\ 0 & \text{elsewhere} \end{cases} \quad (4)$$

and

$$s_{BOC(6,1)}(t) = \begin{cases} \text{sign}[\sin(12\pi/T_C)] & 0 \leq t \leq T_C \\ 0 & \text{elsewhere} \end{cases} \quad (5)$$

Therefore, the signal on the E1 data channel can be expressed as:

$$s_{E1}^{dx}(t) = x_{E1}(t) \cdot \left[\sqrt{\frac{\rho-\gamma}{\rho}} s_{BOC(1,1)}(t) + \sqrt{\frac{\gamma}{\rho}} s_{BOC(6,1)}(t) \right] \quad (6)$$

where $x_{E1}(t)$ is the code spreading sequence for the pilot channel whilst it is the product of the navigation message and the code for the data channel. The parameters γ and ρ can be opportunely selected in order to obtain a specific MBOC(6,1,1/11) from different power splits of data and pilot channels. The MBOC(6,1,1/11) selected for Galileo can be obtained for example by implementing a CBOC(6,1,1/11) with a 50%/50% power split between pilot and data component. However, the same MBOC(6,1,1/11) power spectrum can be realized with a CBOC(6,1,4/33) just on the pilot channel and a BOC(1,1) on the data component and a power split repartition between pilot and data of 75%/25%.

The resulting increase of power towards the higher frequency components result in a sharper correlation function with respect to the baseline BOC(1,1). The

normalized autocorrelation functions of the CBOC(6,1,1/11) and CBOC(6,1,4/33) are compared to the BOC(1,1) correlation in Figure 2.

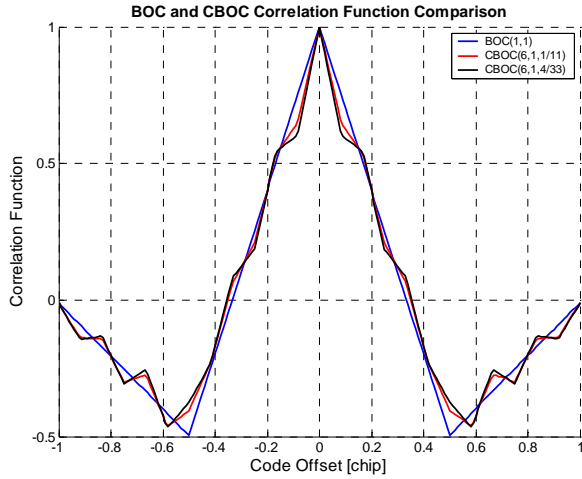


Figure 2 Normalized Autocorrelation Functions comparison of BOC(1,1) (black line), CBOC(6,1,1/11) (red line) and CBOC(6,1,4/33) (blue line) computed for not filtered signals

Larger is the contribution of the BOC(6,1) in the CBOC implementation, sharper is the peak of the correlation function. This characteristic will be deeply highlighted in the following sections in terms of its impact on the signal performance both on the signal acquisition and tracking stages of the receiver.

It is possible to derive, starting from Equation (6), that the CBOC autocorrelation function can be rewritten by means of the BOC(1,1) and BOC(6,1) autocorrelation and cross-correlation functions as:

$$R_{CBOC(6,1,\gamma/\rho)}(\tau) = \frac{\rho-\gamma}{\rho} R_{BOC(1,1)}(\tau) + \frac{\gamma}{\rho} R_{BOC(6,1)}(\tau) + 2 \frac{\gamma}{\rho} \sqrt{\frac{\rho-\gamma}{\gamma}} R_{BOC(1,1)BOC(6,1)}(\tau) \quad (7)$$

where the term $R_{BOC(1,1)BOC(6,1)}(\tau)$ is the cross-correlation term between the BOC(1,1) and BOC(6,1). The presence of such a cross-correlation factor in Equation (7) shows that the CBOC implementation leads just to an approximation of the MBOC spectrum as defined in Equation (3). Lower is the amplitude of the cross term, closer is the overall spectrum with respect to the desired one.

It has to be remarked how the different choices of the parameters γ and ρ produce different correlation functions (as depicted in Figure 2) and then how different performances in acquisition and tracking are expected for different CBOC solutions.

IV. ACQUISITION OF THE OPTIMIZED CBOC SIGNAL

The first operation performed by any GNSS receiver is the signal acquisition, that is in charge of understanding which satellites are in the line of sight and providing the tracking stages with a coarse estimation of the received code delay together with a rough estimation of the Doppler frequency shift.

The declaration of the presence or absence of a satellite and the determination of both code delay and Doppler shift are obtained by evaluating a two dimensional matrix called search space. Each item of such a matrix corresponds to the value assumed by the bi-dimensional correlation function for a specific couple of code delay $\hat{\tau}$ and Doppler shift \hat{f}_d . In this paper, one of the main tasks is to test the performance of the new modulations employing the same acquisition engines as in the case of the BOC(1,1).

As shown in [4] there are several solutions for the signal acquisition that can be found in literature: serial search, fast acquisition and parallel acquisition in frequency domain. All these techniques only differ in the way the search space is obtained, but they are equivalent in terms of performance if compared under the same working conditions. Generally, on top of all the other features, any acquisition strategy is completely characterized once the triple false alarm probability, detection probability and carrier to noise ratio is identified.

The false alarm probability is defined as the probability that the signal is declared present in a wrong cell, while the detection probability is the probability that a signal is detected under the condition of perfect code delay and Doppler shift alignment.

The false alarm probability can be easily derived considering the signal belonging to a wrong satellite or in misalignment conditions as the integral of the tail of a Gamma distribution [7], expressed by:

$$f_{na}^K(r) = \frac{r^{K-1}}{2^K (K-1)! \sigma^{2K}} e^{-\frac{r^2}{2\sigma^2}} u(r) \quad (8)$$

where N is the number of samples coherently integrated, K the non-coherent post accumulations, $\sigma^2 = E\left\{\left(x_{EI}^{loc}[n] \cdot n_w[n]\right)^2\right\}$ the variance of the correlator output branch due to the Gaussian noise affecting the received signal $n_w[n]$. The shape of the correlation function does not affect the false alarm probability, then the same analysis for the threshold setting, V^t , derived in [7] applies for the new signal modulations, as well. The false alarm probability is then:

$$P_{fa}(V_t^t) = \int_{V_t^t}^{+\infty} f_{na}^K(x) dx \quad (9)$$

Under the hypothesis of perfect code and Doppler alignment it is possible to show that the probability density function of the correlator output is [7]:

$$f_a^K(r) = \frac{\sqrt{K}\alpha}{\sigma^2} \left(\frac{r}{\sqrt{K}\alpha}\right)^K e^{-\frac{1}{2}\left(\frac{r^2+K\alpha^2}{\sigma^2}\right)} I_{K-1}\left(r\frac{\sqrt{K}\alpha}{\sigma^2}\right) \quad (10)$$

being $\alpha = \sqrt{E_{Rx}} N/2$ a term proportional to the power of the digitized signal $x_{E1}^{rx}[n]$. Finally, the detection probability is the integral over the tail of $f_{aR}^K(r)$ is [8]:

$$P_d(V_t) = \int_{\sqrt{V_t}/\sigma}^{+\infty} f_{aR}^K(x) dx = Q_K\left(\frac{\alpha}{\sigma}, \frac{\sqrt{V_t}}{\sigma}\right) \quad (11)$$

The detection law for an acquisition system is derived supposing the system able to perfectly recover the code delay and the Doppler frequency shift. However, in real applications, these conditions are rarely verified. Neither the code delay nor the Doppler shift are exactly in the set of delays and frequencies used in the search space evaluation. This condition is cause of additional impairments, or losses, which reduce the amplitude of the correlation peak used in acquisition.

The two-dimensional correlation function can be locally approximated as the product of correlation along the delay axis and Doppler axis [7]

$$R(\Delta f_d, \Delta \tau) = R_{Doppler}(\Delta f_d) R_{Code}(\Delta \tau) \quad (12)$$

where Δf_d and $\Delta \tau$ are the Doppler shift and code phase error respectively. The total loss contribution can be then analyzed separately Since it just becomes the product of these two impairments.

As far as the code loss is concerned the reduction of the correlation output used for the signal acquisition can be accounted in the logarithmic way as:

$$\alpha_{loss}|_{dB} = 20 \log |R_{Code}(\tau)|. \quad (13)$$

A plot of this relation for the CBOC(6,1,1/11), CBOC(6,1,4/33) and the BOC(1,1) is reported in Figure 3

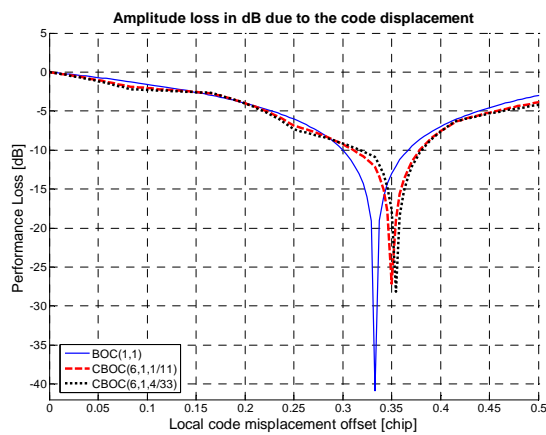


Figure 3 Performance Loss as a function of the code offset for the BOC(1,1), CBOC(6,1,1/11) and CBOC(6,1,4/33)

As in the case of correlation loss due to the code phase offset, the Doppler phase error encountered in the acquisition process produces a reduction of the correlation peak that is demonstrate in [7] to be equal to:

$$\beta_{loss}|_{dB} \cong 20 \log_{10} |D_N[\pi(f_d - \hat{f}_d)]| \quad (14)$$

being $D_N(\omega/2) = \frac{\sin(\omega N/2)}{N \sin(\omega/2)}$ the Dirichlet function. This

amplitude loss is depicted in Figure 4, where the integration time goes from $T = 4$ ms to $T = 12$ ms with 4 ms of step and the Doppler search step is consequently reduced from $\Delta f_d = 250$ Hz to $\Delta f_d = 83.33$ Hz.

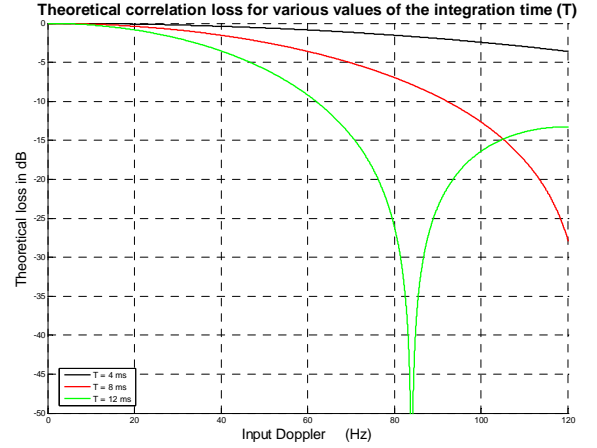


Figure 4 Logarithmic Doppler Loss

In order to consider the different losses correctly, the probability distribution of the code phase offset and Doppler shift, considered as random variables, have to be modeled. The resolution used in the acquisition phase is usually of some integer fraction $\pm 1/L$ of chip/slot and therefore the maximum absolute phase offset $\Delta \tau$ can be assumed uniformly distributed between $\pm 1/(2L)$ chip/slot; the Doppler frequency Δf_d can be assumed to be uniformly distributed between zero and half the maximum absolute frequency bin width.

The combined loss due to the two independent effects is the sum of the contributions of the two losses. Thus, according to the definition of [4] and [7], the detection probability including the code phase offset and Doppler frequency shift loss effect is:

$$P_d = 2N \int_{-1/2L}^{1/2L} \int_{-1/2N}^{1/2N} Q_k \left(\frac{\sqrt{k}\alpha}{\sigma} R(f, \theta), \frac{\sqrt{V_t}}{\sigma} \right) df d\theta \quad (15)$$

with $R(f, \theta) = D_N(\pi f) R_{Code}(\theta)$.

The acquisition performance can be depicted by means of the so called Receiver Operative Characters (ROC) graphs where the detection probability is reported versus the false alarm probability. This is the case of Figure 5 where a comparison among the CBOC(6,1,1/11) and the CBOC(6,1,4/33) is addressed for different code search step resolutions for a Carrier to Noise Ratio C/N_0 of 35 dBHz and a single code period integration time.

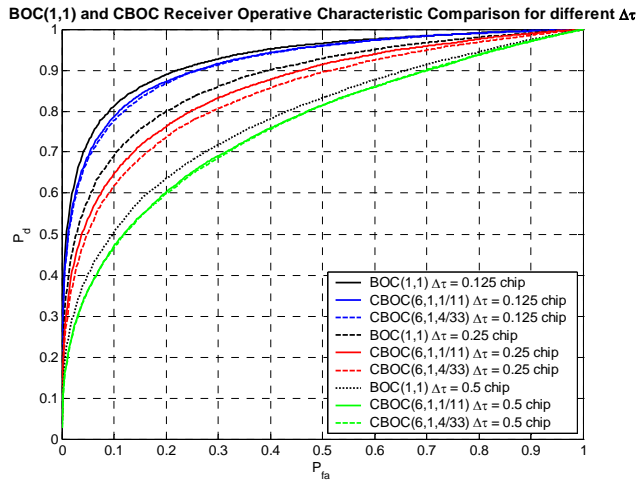


Figure 5 Receiver Operative Characteristic comparison among different CBOC implementations and BOC(1,1) for different $\Delta\tau$ at a C/N_0 of 35 dBHz.

It is clear that reducing the code search step resolution higher detection probabilities can be achieved for the same false alarm probabilities, since lower correlation losses are expected. This come at the cost of having more correlation points to be evaluated and then longer acquisition time. For the same resolution $\Delta\tau$, the CBOC(6,1,1/11) slightly outperforms the CBOC(6,1,4/33): again a key role is played by the shape of the correlation function which is directly connected to the acquisition losses. Because the CBOC(6,1,4/33) presents a sharper correlation function, for the same step resolution $\Delta\tau$, larger correlation losses must be expected thus lower average detection probabilities are obtained, as proved by the Monte-Carlo simulation of Figure 5.

Another possibility to highlight and to show the acquisition performance is given by graphs which depict the detection performance for a given false alarm probability versus the received channel Carrier to Noise Ratio C/N_0 . Figure 6 compares different CBOC implementations for different code search step resolutions.

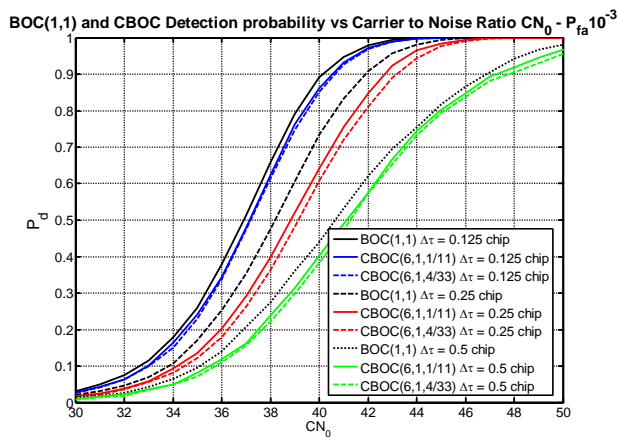


Figure 6 Detection probability versus the Carrier to Noise ratio at a false alarm probability of 10^{-3} . Comparison among different CBOC implementations for different Search Space resolutions

Similar considerations can be made from the analysis of Figure 6, where it is possible to see that better detection performance are obtained generally with the CBOC(6,1,1/11) and with smaller code search steps.

In order to better address the performance of the new modulations a comparison of the acquisition performance of the CBOC modulations with the baseline BOC(1,1) modulation must be performed. Looking at Equation (14) and (15) and to Figure 4, it is easy to understand that the Doppler contributes in the same way to reduce the correlation peak in the search space both for the BOC(1,1) and the CBOC. The only difference is the shape of the correlation function. Considering that the BOC(1,1) correlation function is wider than those of the CBOC implementations, according to Figure 3, a lower code loss should be expected for the BOC(1,1).

In fact, it is possible to see again in the performance graphs of Figure 5 and Figure 6 that the BOC(1,1), for the same signal power, always outperforms the CBOC modulations.

It has not to be forgotten that one of the aims of the CBOC modulations is to maintain the interoperability and the compatibility with the existing systems. In fact the contribution of the BOC(1,1) in the CBOC definition (see Equation (6)) still assures a non zero cross-correlation function between CBOC and BOC(1,1).

Figure 7 reports the correlation functions obtained demodulating the CBOC with a local BOC(1,1) code. This might be the working scenario of a BOC(1,1) legacy receiver which has to deal with the new optimized signal. As it is well shown in Figure 7, the cross-correlation functions of the CBOC modulations and the BOC(1,1) are quite similar to the pure BOC(1,1) correlation function. They are mainly characterized by a reduction of the peak maximum due to the cross loss given by the BOC(6,1) presence in the CBOC, but the correlation slope and widths are practically comparable.

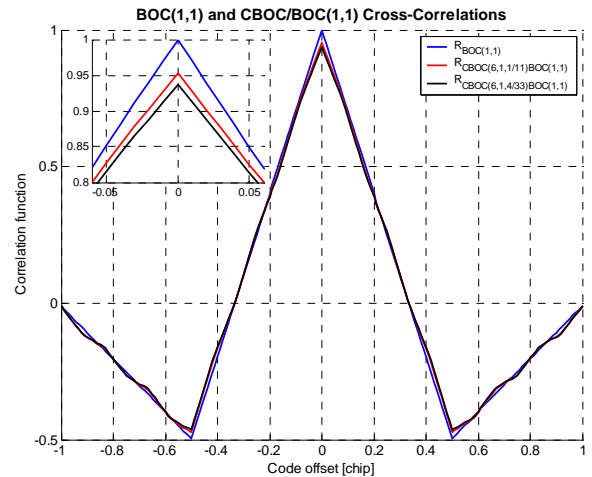


Figure 7 BOC(1,1) and CBOC cross-correlation functions comparison computed over an infinite bandwidth and zoom of correlation peaks

It is then likely to be able to acquire and track the new proposed signals with a BOC(1,1) legacy receiver, with a minimal degradation of performance.

By looking at the shape of the cross-correlation functions of $R_{CBOC(6,1,1/11)BOC(1,1)}$ and $R_{CBOC(6,1,4/33)BOC(1,1)}$ it is

likely that the correlation loss in the acquisition phase can be mainly attributed to the correlation maxima reduction and not quite significantly due to the correlation slope. This is the case of the ROC curves reported in Figure 8 where the performance of the CBOC(6,1,1/11) demodulated by means of a BOC(1,1) replica is reported together with the performance of the standalone BOC(1,1) and CBOC(6,1,1/11).

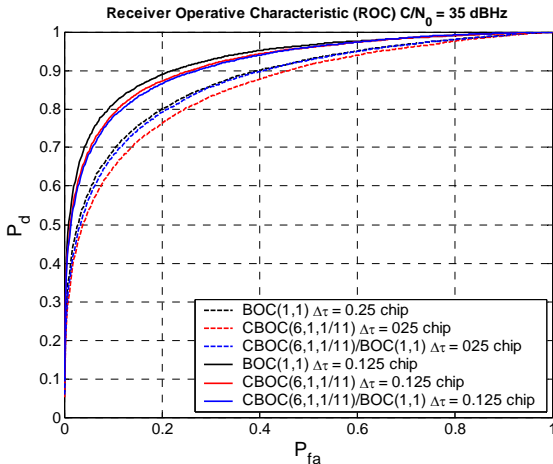


Figure 8 Receiver Operative Characteristic comparison, at a C/N_0 of 35 dBHz using different $\Delta\tau$. Comparison for the pure BOC(1,1), CBOC(6,1,1/11) and the CBOC(6,1,1/11) demodulated with a BOC(1,1) replica

The comparison is made considering a code delay step of 0.25 and 0.125 chip. The detection probability for a false alarm probability of 10^{-3} versus the Carrier to Noise Ratio, is reported in Figure 9.

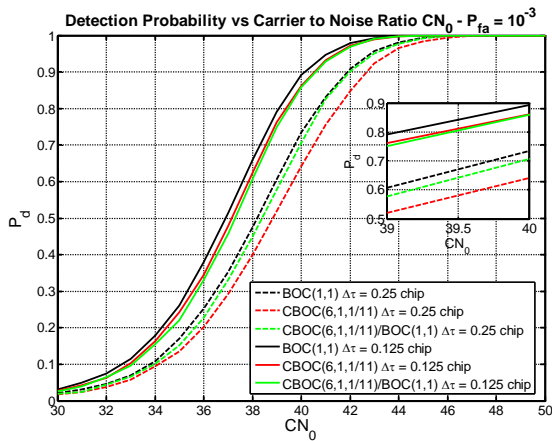


Figure 9 Detection probability versus the C/N_0 at a false alarm probability of 10^{-3} . Comparison among pure BOC(1,1), CBOC(6,1,1/11) and the CBOC(6,1,1/11) demodulated with a BOC(1,1) replica

It is interesting to notice how, when the search space is built with a code step of 0.25 chip, higher detection probabilities can be obtained by demodulating the CBOC(6,1,1/11) with a local BOC(1,1) implementation. When the code step used in the search space is reduced to 0.125 chip than the solution to demodulate the CBOC(6,1,1/11) with a local BOC(1,1) does not outperform the pure CBOC(6,1,1/11) solution.

Similar considerations can be made for the case of the CBOC(6,1,4/33) relative to ROC and Carrier to Noise Ratio graphs of Figure 10 and Figure 11.

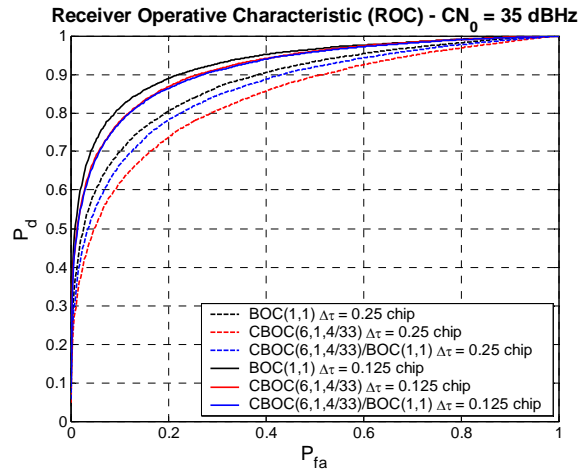


Figure 10 Receiver Operative Characteristic comparison, at C/N_0 of 35 dBHz and different spacing, for the standalone BOC(1,1) and CBOC(6,1,4/33) and the CBOC(6,1,4/33) demodulated with a BOC(1,1) replica

The better performance of the CBOC demodulated by means of a BOC(1,1) for a certain acquisition code search step $\Delta\tau$, can be explained considering that the cross-correlations $R_{CBOC(6,1,1/11)BOC(1,1)}$ and $R_{CBOC(6,1,4/33)BOC(1,1)}$ are quite similar to the $R_{BOC(1,1)}$ and they differ mainly from it for a reduction of the maximum peak. For a certain $\Delta\tau$ detection probability takes more advantage by the sharper CBOC correlation with respect to the reduction induced on the maximum peak. When $\Delta\tau$ is small enough, the loss given by a sharper correlation function becomes less important and this explains the better performance of the pure CBOC when $\Delta\tau$ is for example 0.125 chip.

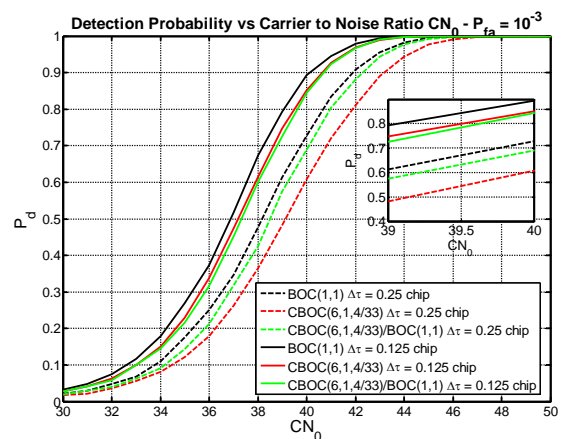


Figure 11 Detection probability versus the C/N_0 at a false alarm probability of 10^{-3} Comparison among pure BOC(1,1), CBOC(6,1,4/33) and the CBOC(6,1,4/33) demodulated with a BOC(1,1) replica

In fact, analyzing Equation (15), the integral operator, somehow, averages the detection probability with the

shape of the correlation function, which thus plays a wider role.

V. TRACKING PERFORMANCE OF THE OPTIMIZED SIGNAL

Several different parameters can be considered during the optimization process of a GNSS signal waveforms. Among all one of the most important characteristics in this process is the improvement of the tracking and multipath performance.

The ability of the tracking loop to mitigate thermal noise can be assessed using the Cramer-Rao lower bound in presence of white noise. The tracking jitter standard deviation σ_{LB} can be written as [6]:

$$\sigma_{LB} = \frac{1}{2\pi\beta_{RMS}} \sqrt{\frac{B_L}{\lambda \frac{C}{N_0}}} \quad (16)$$

where B_L is the DLL one-sided bandwidth, $\frac{C}{N_0}$ is the carrier-to-noise ratio and β_{RMS} is the Root Mean Square bandwidth (RMS) defined as:

$$\beta_{RMS} = \sqrt{\frac{\int_{-\infty}^{\infty} f^2 \frac{H(f)G(f)}{\int_{-\infty}^{\infty} H(f)G(f)df} df}{\int_{-\infty}^{\infty} H(f)G(f)df}} \quad (17)$$

The term $G(f)$ is the signal PSD and $H(f)$ is the front-end transfer function. The RMS bandwidth measures the frequency extension of a signal and it is a good metric to compare the optimality of different signal modulations, in fact bigger is the term β_{RMS} in Equation (16) lower is the tracking jitter.

Figure 12 shows the comparison among the BPSK, BOC(1,1), MBOC(6,1,1/11) and MBOC(6,1,4/33) spreading modulations for a given receiver bandwidth assumed to have a rectangular shape. It is easy to notice that for a signal bandwidth lower than about 12 MHz the MBOC modulations do not produce any advantage with respect to the BOC(1,1) but β_{RMS} increases significantly when more than 12 MHz bandwidth is adopted.

Figure 13 shows a comparison of the simulated tracking jitter for the different spreading modulations. Simulations of a coherent tracking block with an early-late correlators spacing of 0.1 chip, a one-sided DLL bandwidth of 1 Hz and a receiver bandwidth of 12 MHz have been made to produce the results. The CBOC(6,1,1/11), and CBOC(6,1,4/33) implementations are compared with the classical BOC(1,1) modulation.

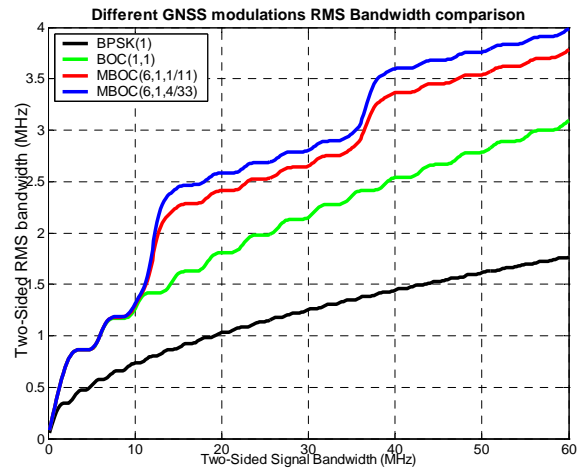


Figure 12 Root Mean Square Bandwidth versus the two sided receiver bandwidth evaluated considering an ideal filter over a bandwidth $\pm B$

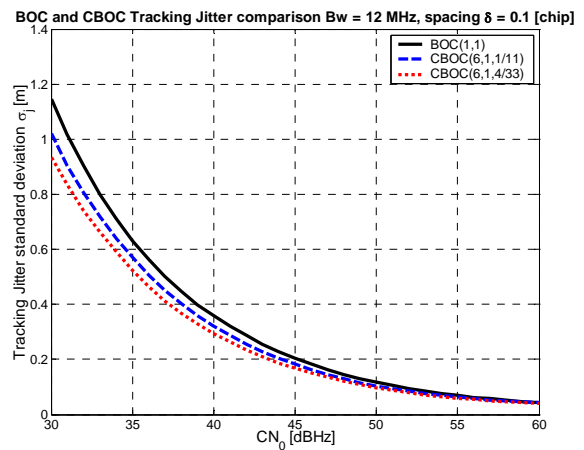


Figure 13 Simulation of the tracking Jitter standard deviation, Coherent EML Discriminator with 0.1 chip spacing and receiver bandwidth of 12 MHz

Simulations confirmed that better performance can be obtained by the new modulations thanks to the higher frequency components in the PSD that lead to narrower autocorrelation function peaks and discrimination functions with higher slopes at the origin.

In order to assess the impact of the CBOC signals on the BOC(1,1) based receivers Figure 14 shows the tracking jitter performance when the CBOC is demodulated with a local BOC(1,1) signal.

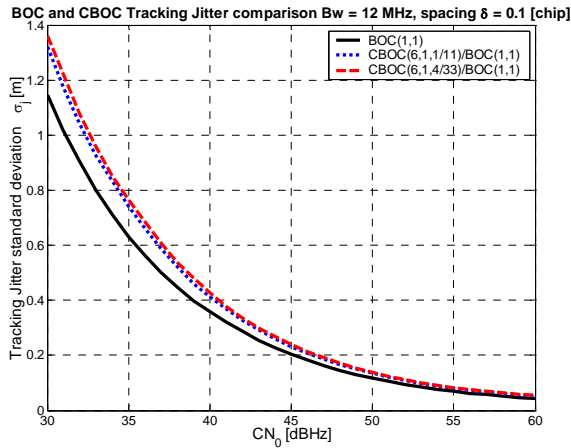


Figure 14 Simulation of the tracking Jitter standard deviation, Coherent early minus late Discriminator with 0.1 chip spacing and legacy BOC(1,1) receiver

As in the case of the acquisition performance, the loss due to the cross-correlation factor between the CBOC and BOC(1,1) signals leads to lower tracking jitter performance with respect to the pure BOC(1,1) solution.

VI. MULTIPATH PERFORMANCE

One of the worst error sources for a navigation receiver is multipath propagation. The most common tool to address the system performance when the received signal is affected by multipath is the tracking error envelope plot. The error envelopes report the tracking bias error of a DLL when the received signal is affected by a single reflected ray.

Figure 15 shows the multipath error envelope curves obtained by the same software receiver output already employed to obtain the tracking jitter curves of Figure 13 and Figure 14, employing a narrow correlator with spacing 0.1 chip..

Once again the results state better performance of the new optimized CBOC signal with respect to the BOC(1,1), due to the sharper correlation peak.

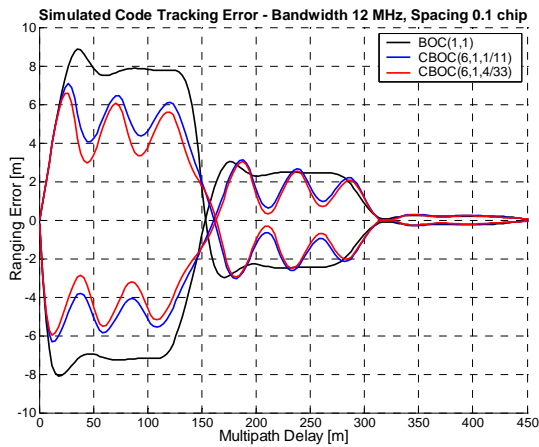


Figure 15 multipath error envelope comparison for BOC(1,1), CBOC(6,1,1/11) and CBOC(6,1,4/33). Receiver bandwidth of 12 MHz (4 pole Butterworth) and 0.1 Early-Late chip spacing

To get a general understanding of the impact of CBOC on a receiver based on the BOC(1,1) modulation, several simulations have been carried out to assess the multipath error envelopes when the CBOC modulation is demodulated with a BOC(1,1) code. Figure 16 shows such a comparison.

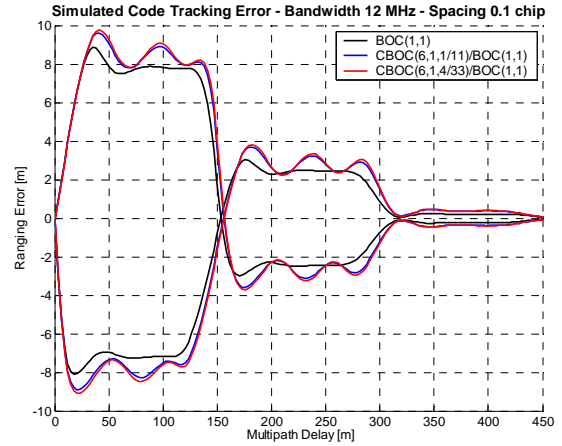


Figure 16 multipath error envelope comparison for BOC(1,1), CBOC(6,1,1/11) and CBOC(6,1,4/33) demodulated with a local BOC(1,1). Receiver bandwidth of 12 MHz (4 pole Butterworth) and 0.1 Early-Late chip spacing

The CBOC signal can improve both the tracking and multipath performance and the compliance with Galileo BOC(1,1) legacy receivers can still be assured, even though some degradations are experienced, as proved in the simulations (see Figure 14 and Figure 16).

To complete the investigation of the E1 optimized signal, it is interesting to see how the system performs when a Strobe discriminator is used.

Figure 17 presents the comparison among the multipath error envelope of the BOC(1,1), CBOC(6,1,1/11) and CBOC(6,1,4/33) with the same receiver set-up as the previous simulations.

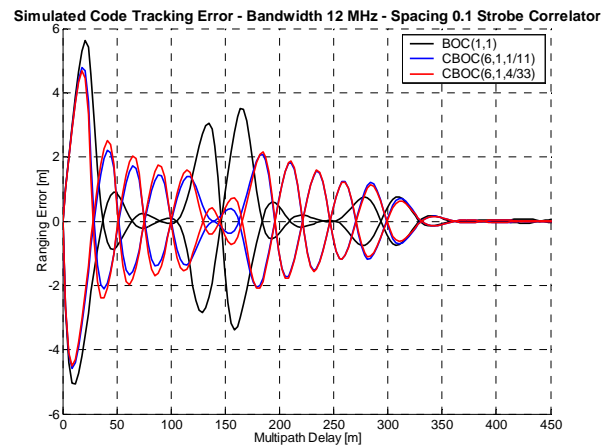


Figure 17 Multipath error envelope comparison for BOC(1,1), CBOC(6,1,1/11) and CBOC(6,1,4/33). Receiver bandwidth of 12 MHz (4 pole Butterworth) and 0.1 Early-Late chip spacing

The situation of an hybrid receiver which operates the CBOC signal with a local BOC(1,1) and employing a Strobe discriminator is reported in Figure 18.

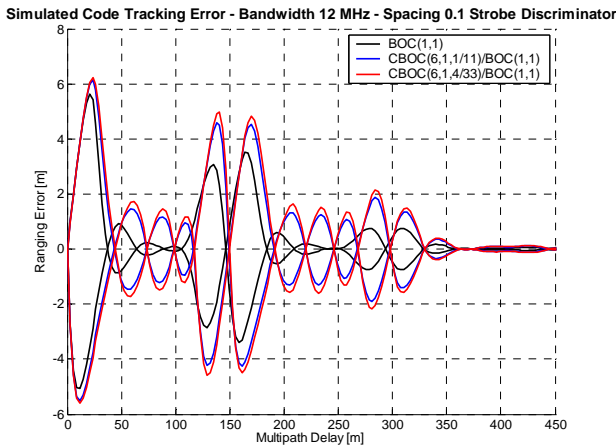


Figure 18 Multipath error envelope comparison for BOC(1,1), CBOC(6,1,1/11) and CBOC(6,1,4/33) demodulated with a local BOC(1,1). Receiver bandwidth of 12 MHz (4 pole Butterworth) and 0.1 Early-Late chip spacing

When the DLL employs a Strobe discriminator, no significant increase of performance seems to be achieved. In fact, the Strobe discrimination functions for the CBOC modulations do not present the “zero regions” as in the case of the BOC(1,1) and then this effect is reflected in the multipath error envelope as shown in Figure 17 and Figure 18.

VII. CONCLUSIONS

According to the recent work of the modernization of the Galileo E1 signals, two are at the moment the proposed signal solutions to implement a MBOC(6,1,1/11) spectrum. This paper is focused on the analysis of the acquisition and tracking jitter performance as well as the multipath error envelope of the CBOC(6,1,1/11) and CBOC(6,1,4/33) solutions.

The paper shows how the shape of the CBOC autocorrelation functions may reduce the detection probability during the signal acquisition. On the other hand the signal tracking can benefit of the sharper CBOC correlation functions achieving better jitter performance.

If the CBOC implementation uses a pure BOC(1,1) on the data channel, a good trade off solution could be to acquire the data channel having then the acquisition performance of a BOC(1,1) but to track the CBOC signal with consequently lower tracking jitters.

If the CBOC will be selected both for the data and pilot channels, then the acquisition might be less performing comparing to same situation with a BOC(1,1). However, this problem could be, somehow, mitigated demodulating the CBOC with a local BOC(1,1) when large values of $\Delta\tau$ are adopted and with a pure CBOC in the other cases aiming at obtaining the lower code loss for that particular code search space resolution.

The paper also presents some results on the impact that the CBOC modulation may infer on the BOC(1,1) legacy receivers. The results proves that a degradation of performance must be expected, but that at the same time it

is absolutely tolerable, especially if they are compared with the benefits that the proposed modulation could introduce at the only cost of employing a wider front-end bandwidth and of a slightly increase in the receiver technology complexity.

REFERENCES

- [1] G. W. Hein, J. Rodriguez, S. Wallner, J. W. Betz, C. J. Hegarty, J. Rushanan, A. L. Kraay, A. R. Pratt, Lt S. Lenahan, J. Owen, J. L. Issler, T. A. Stansel, “MBOC: The New Optimized Spreading Modulation recommended for Galileo L1 OS and GPS L1c”, *InsideGNSS* Vol 1, Number 4, May/June 2006
- [2] <http://gps.losangeles.af.mil/engineering/icwg/Docs/EC%20and%20US%20Joint%20Statement%20on%20GALILEO%20and%20GPS%20Signal%20Optimization%20-%202024%20Mar%2006.pdf>
- [3] <http://pnt.gov/public/docs/2004-US-EC-agreement.pdf>
- [4] Daniele Borio, Maurizio Fantino, Letizia Lo Presti, Laura Camoriano, “Acquisition analysis for Galileo BOC modulated Signals: theory and simulation” *European Navigation Conference (ENC) 2006*, Manchester, UK, May 7-10, 2006
- [5] <http://gps.losangeles.af.mil/engineering/icwg/Docs/WGA%20Signe d%20Recommendation%20on%20MBOC%20%2023%20Mar%2006.pdf>
- [6] J. W. Betz, “Design and Performance of Code Tracking. for the GPS M Code Signal,” *Proceedings of ION GPS-2000*, , September 2000.
- [7] Papoulis, *Probability, random variable and stochastic processes*, 3rd ed. New York: McGraw Hill, 1991.
- [8] Maurizio Fantino, “*Study of Architectures and Algorithms for Software Galileo Receivers*”, PhD Dissertation, Electronic Department - Politecnico di Torino, May 2006
- [9] J. I. Marcum, “A statistical theory of target detection by pulsed radar”, *IEEE Trans. on Information Theory*, pp. 59–267, 1 December 1947.